

# A new approach to the analysis of vessels RTD curves

Sergio P. Ferro, R. Javier Principe and Marcela B. Goldschmit\*

Center for Industrial Research

Córdoba 320

1054, Buenos Aires, Argentina

\* E-mail: [sidgld@siderca.com](mailto:sidgld@siderca.com)

August 23, 2001

## Abstract

Mathematical models for the evaluation of residence time distribution (RTD) curves on a large variety of vessels are presented. These models have been constructed by combination of different tanks or volumes. In order to obtain a good representation of RTD curves, a new volume (called convection diffusion volume) is introduced. The convection-diffusion volume allows the approximation of different experimental or numerical RTD curves with very simple models. An algorithm has been developed to calculate the parameters of the models for any given set of RTD curve experimental points. Validation of the models are carried out by comparison with experimental RTD curves taken from literature and with a numerical RTD curve obtained by three dimensional simulation of the flow inside a tundish.

## I Introduction

The residence time of an element of fluid is the time it spends inside the vessel. Since different elements of fluid spend different times inside the vessel, there is a distribution of residence times for each vessel. The residence time distribution (RTD) gives important information about the behavior of the flow inside the different vessels of the continuous caster. Both experimental and numerical techniques can be employed

to obtain the RTD [1]. In both cases the basic idea is to inject a pulse of a tracer at the entrance of the vessel and analyze the concentration of tracer at the exit as function of time. This function is known as the RTD curve. RTD curves are generally represented in terms of dimensionless variables (to be defined in the following section) and typically take the shape of the curve depicted in Figure 1.

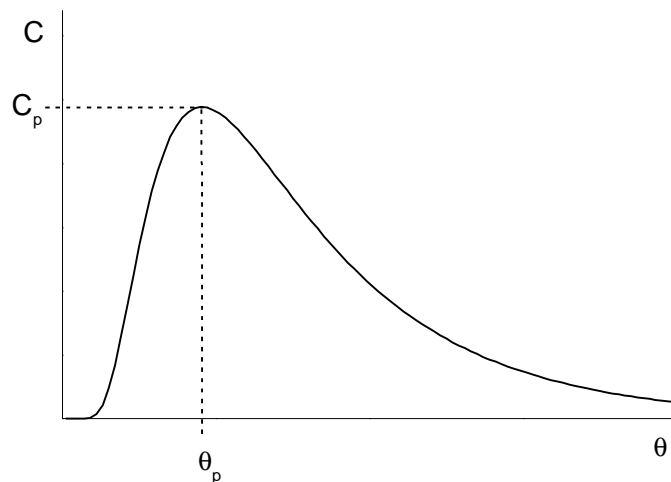


Fig. 1: Typical RTD curve.

Experimental RTD curves are obtained in water models by the injection of a salt solution or a dye as a tracer. In the former case the concentration at the exit of the vessel is obtained by measuring the conductivity of the fluid. In the latter, colorimetry or spectrophotometry techniques are used to get the concentration.

RTD curves can also be obtained by numerical methods. In this case the first step is to calculate the turbulent flow inside the vessel. Different techniques could be applied to solve the steady state turbulent Navier-Stokes equations. The  $k-\epsilon$  method, where  $k$  is the turbulent kinetic energy and  $\epsilon$  is the turbulent kinetic energy dissipation rate, is the most popular [2]. Once the velocity distribution inside the vessel is obtained, the addition of tracer needs to be numerically simulated. A turbulent convection diffusion equation for the concentration of tracer must be solved. A narrow step function has to be imposed at the entrance as boundary condition to simulate the tracer pulse injection. The RTD curve is the concentration of tracer at the exit of the vessel as function of time.

A different approach to the analysis of residence times inside vessels is the numerical modeling by tanks

or volumes [3]. In these models the vessel is divided into different regions (the tanks or volumes) where the flow is supposed to behave in a very simple way. For each volume, the concentration evolves according to a specific differential equation. The models presented in this paper are based on this method.

The numerical modeling of the flow inside vessels by tanks or volumes is widely used in literature, as described in an extensive review published by Mazumdar and Guthrie [1]. Many of these works present models obtained by combinations of mixing volumes, plug flow volumes and dead volumes [3]. However, a good description of RTD curves in terms of these models (called mixed flow models) is not always possible. To improve the accuracy of the models, different modifications were introduced. Martin [4], for instance, proposed a modification of the tank in series model (where the system is divided in several identical mixing volumes) by considering a non-integer number of tanks. Sahai and Ahuja [5], on the other hand, introduced the use of dispersed plug flow volumes instead of the standard plug flow volumes in their study of tundish RTD curves.

The dispersed plug flow volume is based on the dispersion model introduced by Levenspiel and Smith [6] in the chemical reactor analysis, and represents a deviation from the ideal plug flow caused by a longitudinal mixing. In the dispersion model the evolution of tracer concentration in any vessel is modeled by the one dimensional transient convection-diffusion equation. Dispersion models describe accurately the mixing process if the diffusivity is small, but are deficient when diffusivity is large [3], [7].

In Section IV we introduce a new kind of volume named convection-diffusion volume. This volume is also based on dispersion models and is able to describe RTD curves in vessels with any amount of diffusion. We comment the physical interpretation of this new convection-diffusion volume and explain its difference with the dispersed plug flow volume. In Section III we propose a simple model consisting of a single convection-diffusion volume and a dead volume; experimental RTD curves found in literature are analyzed in terms of this model. In order to represent two peaked RTD curves, another model is proposed in Section IV, which consists of two convection diffusion volumes and a dead volume. This model is also used to analyze experimental data, specially two peaked RTD curves. In Section V we present a three dimensional numerical analysis of a four line tundish and the interpretation of its RTD curves in terms of the model described in Section IV. The last section is devoted to conclusions.

## II Convection-Diffusion volumes

### A Basic equations

Let's consider a system with a volume  $V$  of fluid. The fluid enters and exits the system at a flow rate  $Q$ . At the entrance of this system a tracer is being injected and we want to describe the concentration of tracer at the exit. A convection-diffusion one dimensional equation model is used to represent the evolution of concentration of tracer inside the volume,

$$\frac{\partial C(x; \mu)}{\partial \mu} + \frac{\partial C(x; \mu)}{\partial x} = \frac{1}{Pe} \frac{\partial^2 C(x; \mu)}{\partial x^2}; \quad (1)$$

where  $C(x; \mu)$  is the dimensionless tracer concentration and  $x$  and  $\mu$  are the dimensionless time and position expressed in terms of the length of the domain,  $L$ ; and the theoretical residence time  $\tau = \frac{V}{Q} = \frac{L}{v}$  ( $v$  is the velocity inside the domain, assumed constant).  $Pe$  is the turbulent Péclet number,  $Pe = \frac{vL}{D}$ , where  $D$  is the turbulent diffusivity.

We want to solve this equation for all  $0 < x < 1$  and  $\mu > 0$  according to the following initial and boundary conditions,

$$\begin{aligned} C(x; 0) &= 0 \\ C(0; \mu) &= C_0(\mu) \end{aligned} \quad (2)$$

where  $C_0(\mu)$  is any given function of time.

The solution of Eq. (1) which satisfies conditions (2) and does not diverge for large values of  $x$ , is

$$C(x; \mu) = \int_0^{\mu} K_{Pe}(x; \mu - \tau) C_0(\tau) d\tau$$

where the kernel  $K_{Pe}(x; \mu)$  is defined by

$$K_{Pe}(x; \mu) = x \frac{Pe}{4 \sqrt{\pi} \mu^3} \exp\left[-i \frac{Pe(x - \mu)^2}{4\mu}\right]$$

The kernel satisfies the differential equation, the initial condition and the integral property  $\int_0^{\infty} K_{Pe}(x; \mu) d\mu = 1$  for all  $x > 0$ . Since the kernel vanishes at  $x = 0$  for all  $\mu > 0$ ; the boundary condition for the kernel may be written as  $K_{Pe}(0; \mu) = \delta(\mu)$ , where  $\delta(\mu)$  is Dirac's delta function. From these properties of the kernel it is possible to show that  $C(x; \mu)$  satisfies Eq. (1) with conditions (2).

We are interested in the concentration of tracer at the outlet of volume  $x = 1$ :

$$C(1; \mu) = \int_0^\mu K_{Pe}(1; \mu; \zeta) C_0(\zeta) d\zeta \quad (3)$$

with  $K_{Pe}(1; \mu)$  given by

$$K_{Pe}(1; \mu) = \frac{r}{4\mu^3} \frac{Pe}{Pe} \exp\left[-\frac{Pe(1-\mu)^2}{4\mu}\right] \quad (4)$$

Now, we introduce the convection-diffusion volume defined by its volume  $V$  and its Péclet number  $Pe$ : In this volume, if the concentration at the entrance  $C_0(\mu)$  and the flow rate  $Q$  are given, the concentration at the exit is calculated from Equation (3):

## B Physical interpretation

From the properties described in the preceding section we can observe that, if  $C(0; \mu) = \delta(\mu)$ ; then  $C(1; \mu) = K_{Pe}(1; \mu)$ . Consequently, the kernel  $K_{Pe}(1; \mu)$  may be regarded as the tracer concentration leaving the system, when a pulse of concentration is injected at the system entrance at  $\mu = 0$ .

The convolution integral in Eq. (3) indicates that the outcoming concentration at time  $\mu$  is influenced by the whole history of the concentration at the entrance previous to time  $\mu$ . Also, since the kernel at time  $\mu$  is the response of the system to a pulse of concentration at the entrance at time  $\mu = 0$ ,  $C(1; \mu)$  may be considered as the response of the system to a series of pulses of amplitude  $C(0; \zeta) d\zeta$  injected at the entrance at time  $\zeta$ .

The set of equations described in the previous section were deduced under the assumption of open system. That is, the diffusivity is considered continuous across the input - output boundaries of the system [7].

The Péclet number indicates how diffusive the flow in the system is.

<sup>2</sup> The limit  $Pe \rightarrow 1$  corresponds to purely convective flow with no diffusion. In this limit  $K_{Pe}(1; \mu) \rightarrow \delta(1 - \mu)$  and  $C(1; \mu) \rightarrow C(0; 1 - \mu)$ . This is the expected solution for the concentration of tracer in a system with no diffusion, that is, a plug flow system.

<sup>2</sup> On the other hand, when  $Pe \rightarrow 0$ ; diffusion is very large and the concentration at the entrance propagates instantaneously along the volume. The function  $K_{Pe}(1; \mu)$  presents a sharp peak near

$\mu = 0$  vanishing anywhere else and  $C(1; \mu) \neq C(0; \mu)$ : This result contrasts with the large diffusivity limit for closed systems  $C(1; \mu) \neq \int_0^1 e^{i(\mu - \zeta)} C_0(\zeta) d\zeta$  [7].

Let's analyze the behavior of  $C(1; \mu)$  in a convection-diffusion volume when a pulse is injected at the entrance. In this case  $C(1; \mu) = K_{Pe}(1; \mu)$  is the RTD curve of a system represented by a single convection-diffusion volume. Since  $C(1; 0) = 0$  (initial condition, Eq. (2)) and  $C(1; \mu) \neq 0$  as  $\mu \neq 1$  (from Eq. (4)), the curve must reach a maximum value  $C_p$  at a certain time  $\mu_p$ : The general appearance of such a curve has already been shown in Figure 1. The values of  $\mu_p$  and  $C_p$  are given by

$$\mu_p = \frac{1 + 3 + \frac{Pe}{9 + Pe^2}}{Pe} \quad (5)$$

and

$$C_p = C(1; \mu_p) = \frac{S}{4 \frac{1}{4} \mu_p^3} \exp \left[ -i \frac{Pe(1 - \mu_p)^2}{4 \mu_p} \right]$$

The first expression shows that  $\mu_p \neq 0$  when  $Pe \neq 0$  and  $\mu_p \neq 1$  when  $Pe \neq 1$ . That is, in the limit of perfectly mixed flow ( $Pe \neq 0$ ) the peak is at  $\mu = 0$ ; since the concentration behaves as  $\pm(\mu)$ : For larger values of the Péclet number,  $\mu_p$  increases. When the flow is dominated by convection  $\mu_p$  approaches the unity and in the limit of pure plug flow  $\mu_p = 1$ ; in agreement with the fact that, in this limit, the concentration tends to  $\pm(1 - \mu)$ : In consequence the Péclet number can be estimated from the position of the RTD curve peak,

$$Pe = \frac{6 \mu_p}{1 - \mu_p^2} \quad (6)$$

## C Comments on boundary condition

It is important to note that the dispersion model of Levenspiel and Smith makes use of a rather different function to describe the response of the system to a pulse injected at the entrance [6],

$$k_{Pe}(x; \mu) = \frac{r}{4 \frac{1}{4} \mu} \exp \left[ -i \frac{Pe(x - \mu)^2}{4 \mu} \right] = \frac{\mu}{x} K_{Pe}(x; \mu)$$

The kernel  $k_{Pe}(x; \mu)$  was obtained from a different solution of Eq. (1) (see reference [6]). At the entrance, this kernel does not represent a pulse, since it does not vanish for  $\mu > 0$ ,

$$k_{Pe}(0; \mu) = \frac{r}{4 \frac{1}{4} \mu} \exp \left[ -i \frac{Pe \mu}{4} \right]$$

In Figure 2, the function  $K_{Pe}(0; \mu)$  is plotted as function of  $\mu$  for different values of the parameter  $Pe$ : For large values of the Péclet number (i.e. if diffusion is low) the concentration decreases rapidly away from  $\mu = 0$  and in the limit  $Pe \rightarrow \infty$ ,  $K_{Pe}(0; \mu)$  tends to form of a pulse. However, for general values of  $Pe$ ,  $K(0; \mu)$  presents long tails. This means that the tracer is injected at the entrance of the system during a certain period of time instead of being injected instantaneously at  $\mu = 0$ : The function  $K_{Pe}(x; \mu)$  can be regarded as the response of the system to a pulse at the entrance, but only in the limit of plug flow. It is easy to see that in this limit,

$$K_{Pe}(1; \mu) \approx K_{Pe}(1; \mu) \approx \frac{r}{4} \frac{Pe}{Pe} \exp\left(-\mu \frac{Pe(1-\mu)^2}{4}\right) :$$

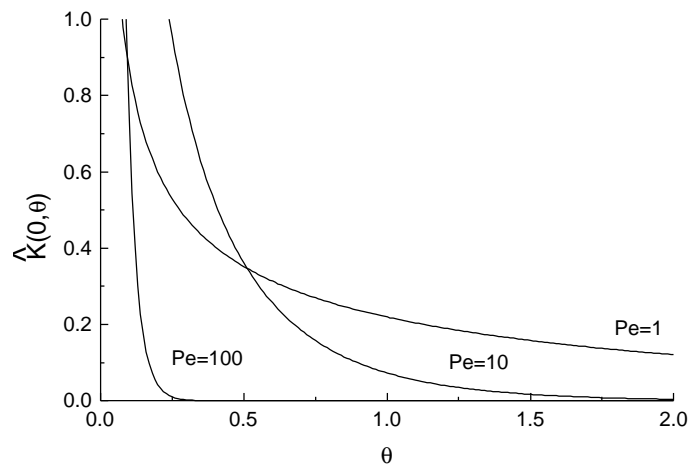


Fig. 2: Concentration at the origin as function of time, for the solution of Eq. (1) described in reference [6]

It is also interesting to compare the average residence times,  $\mu_{av} = \int_0^1 \mu K_{Pe}(1; \mu) d\mu$  and  $\beta_{av} = \int_0^1 \mu K_{Pe}(1; \mu) d\mu$ : It can be seen that  $\beta_{av} = 1 + \frac{2}{Pe}$  (see reference [6]) only remains close to the unity in the limit of plug flow and diverges on the limit of high diffusion. On the other hand,  $\mu_{av} = 1$  for any value of  $Pe$ :

As pointed out in [7], [3] the dispersion model can be used only for systems with relative small degree of mixing. In our belief that the use of the kernel  $K_{Pe}(x; \mu)$  instead of  $K_{Pe}(x; \mu)$  allows the application of the dispersion model to more general situations.

### III A simple vessel model

In this Section we will describe the whole vessel with a very simple model composed by a convection diffusion volume ( $V_a$ : active volume) and a dead volume ( $V_d = V - V_a$ ), to take into account dead or slowly moving flow regions. It is assumed that in the active zone the flow behaves as one dimensional with a characteristic time  $\frac{V_a}{Q}$ . When the concentration at the entrance of the model corresponds to a pulse, the concentration at the exit of the model can be obtained from Eq. (3)

$$C(1; \mu) = \frac{1}{V_a} K_{Pe} \left( 1 - \frac{\mu}{v_a} \right) \exp \left[ - \frac{Pe (v_a - \mu)^2}{4 v_a \mu} \right] \quad (7)$$

which is the mathematical expression for the RTD curve. This curve reaches its maximum when

$$\mu_p = v_a \frac{3 + \sqrt{9 + Pe^2}}{Pe} \quad (8)$$

The model has two dimensionless parameters, the Péclet Number  $Pe$  and the fraction of the active volume  $v_a = V_a/V$ . It is useful to relate these parameters to the values of  $\mu_p$ ,  $C_p$  and  $\mu_{av}$  (where  $\mu_{av} = \int_0^1 \mu C(1; \mu) d\mu$  is the average residence time). The following expressions were obtained,

$$v_a = \mu_{av} \quad (9)$$

$$v_d = 1 - \mu_{av}$$

$$Pe = \frac{6 \mu_p \mu_{av}}{\mu_{av}^2 - \mu_p^2} \quad (10)$$

Then, the parameters of the simple vessel model  $v_a$  and  $Pe$  can be estimated from the values of  $\mu_{av}$  and  $\mu_p$  of an experimental RTD curve.

However, the numerical calculation of  $\mu_{av}$  from experimental curves can be difficult, specially for RTD curves with very long tails. In order to find another way to estimate the parameters of the model, the product  $C_p \mu_p$  is going to be considered. This product does not depend on  $v_a$  and is only function of  $Pe$ :

$$C_p \mu_p = a(Pe) = \frac{Pe}{4 \left( 3 + \sqrt{9 + Pe^2} \right)} \exp \left[ - \frac{Pe (3 + \sqrt{9 + Pe^2})^2}{4 \left( 3 + \sqrt{9 + Pe^2} \right)^2} \right] \quad (11)$$

In a RTD diagram,  $a(Pe)$  represents the rectangular area subtended by the origin and the peak of the curve (see Figure 3) and is a monotonous increasing function of the  $Pe$  (see Figure 4). We found that

$a(Pe) \rightarrow a_0 = 0.154$  when  $Pe \rightarrow 0$ , and that  $a(Pe) \rightarrow \frac{Pe}{4} + \frac{3}{4Pe}$  when  $Pe \rightarrow \infty$ . This asymptotic expression can be inverted to obtain a good estimation of  $Pe$  when the flow has small degree of diffusion,

$$Pe \approx \frac{3}{4} + 2\frac{1}{4} (C_p \mu_p)^2 \left( 1 + \frac{3}{4\frac{1}{4} (C_p \mu_p)^2} \right) \quad (12)$$

For  $Pe > 5$  (which corresponds to  $a > 0.55$ ), the Péclet number can be approximated by this expression with an error smaller than 5%:

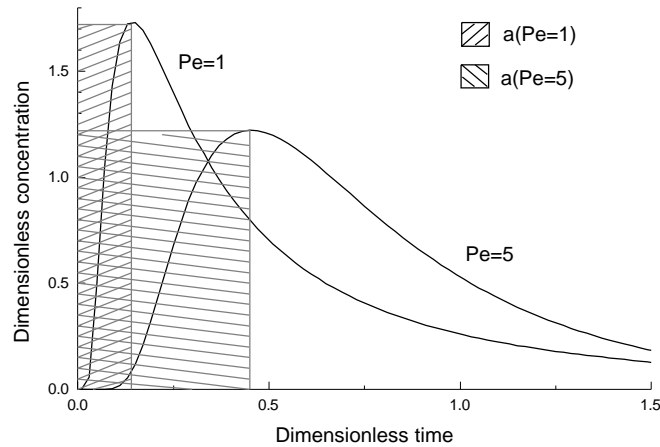


Fig. 3: Relationship between the location of the peak of the RTD curve and the function  $a(Pe)$ .

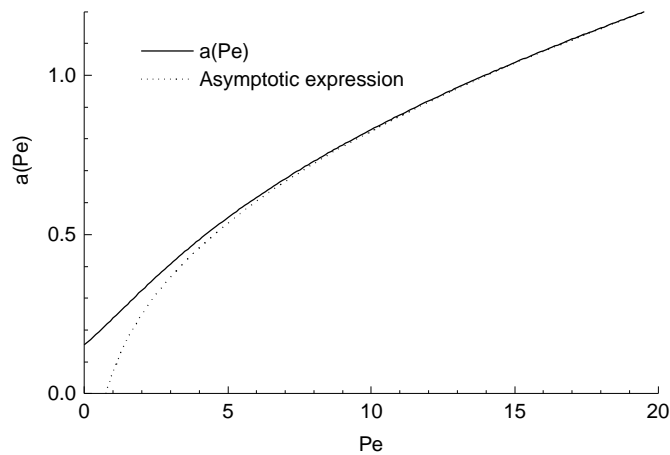


Fig. 4: Function  $a(Pe)$  which relates the Péclet number to the location of the peak of the RTD curve.

Case	1	2
Authors	Barrón-Meza et al	Zong et al.
Reference	[8]	[9]
V [l]	13.7	30.0
Q [l=s]	0.2066	0.0666
type of vessel	one strand tundish	continuous re...ning vessel
Number of Figure	5,6 and 7	8, 9 and 10

Table I: Cases considered for the validation of the simple vessel model.

## A Validation of the simple vessel model

The validation of the simple vessel model proposed in this section was carried out by matching two experimental RTD curves found in literature and described in Table I.

The matching of experimental data was carried out using three different procedures to estimate the parameters  $Pe$  and  $v_a$ ,

Procedure 1: Minimization of the square of the distance between the numerical results of Eq. (7) and the experimental data of the RTD curves, using the Levenberg-Marquardt algorithm. Figures 5 and 8 show the results for this procedure for the two cases described in Table I.

Procedure 2: Numerical estimation of the average residence time using the experimental data and evaluation of  $Pe$  and  $v_a$  using Eq. (10) and Eq. (9). The resulting RTD curves are presented in Figures 6 and 9 for both cases.

Procedure 3: Evaluation of the product  $\mu_p C_p$  from the RTD curve and calculation of  $Pe$  from Figure 4 or from Eq. (11) (in this case a nonlinear equation must be solved using, for example, a Newton Raphson technique) or using the asymptotic expression Eq. (12). Finally  $v_a$  is obtained from Eq. (8). Results are shown in Figures 7 and 10.

The values  $Pe$  and  $v_a$  obtained with the different procedures for both cases are shown in Table II. The procedure 1 provides the best fitting but involves the solution of a nonlinear minimization problem.

Procedure	Parameter	Case1	Case2
1	Pe	5.26	3.64
1	$v_a$	1.0	0.84
2	Pe	4.11	3.77
2	$v_a$	0.97	0.76
3	Pe	4.198	3.02
3	$v_a$	0.96	0.88

Table II: Numerical values of the parameters Pe and  $v_a$

Procedures 2 and 3 give a reasonable estimation of the parameters with very little information from the experimental data. The accuracy of these two procedures depend strongly on the reliability of the evaluation of  $\mu_p$  and  $\mu_{av}$  or  $C_{p_i}$  from the experimental RTD curve.

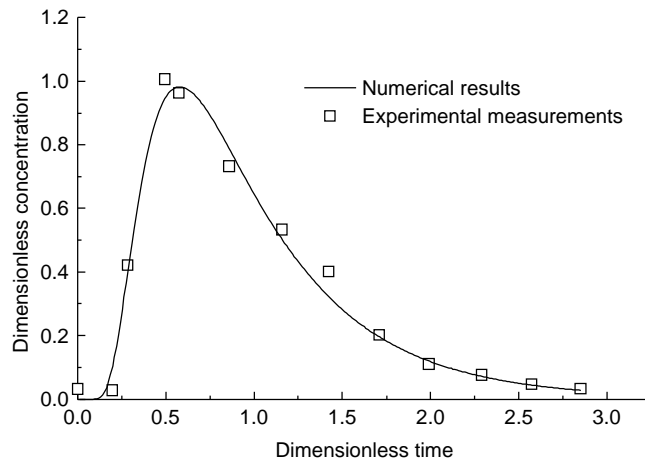


Fig. 5: Comparison of experimental results [8] and the simple vessel model with a least square matching (procedure 1).

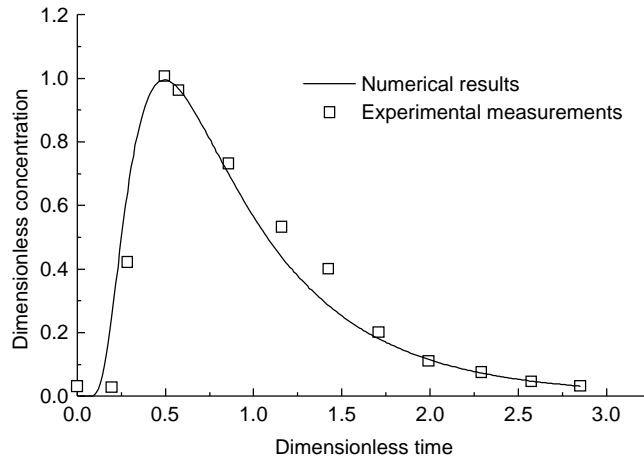


Fig. 6: Comparison of experimental results [8] and the simple vessel model using Eq. (10) and Eq. (9) (procedure 2).

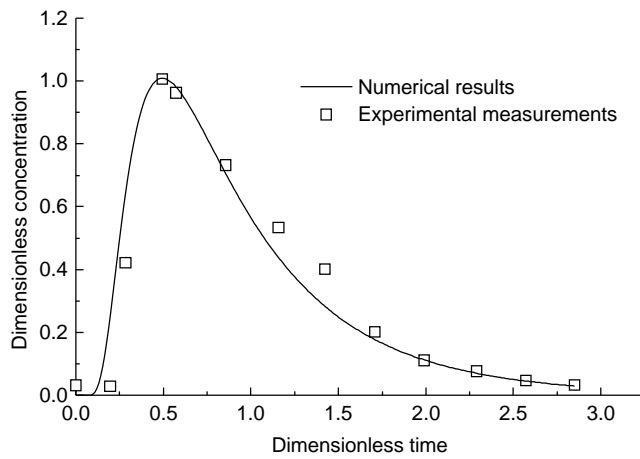


Fig. 7: Comparison of experimental results [8] and the simple vessel model using Eq. (11) and Eq. (8) (procedure 3)

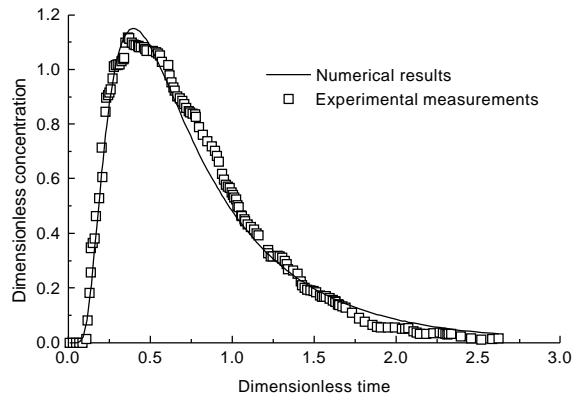


Fig. 8: Comparison of experimental results [9] and the simple vessel model with a least square matching (procedure 1).

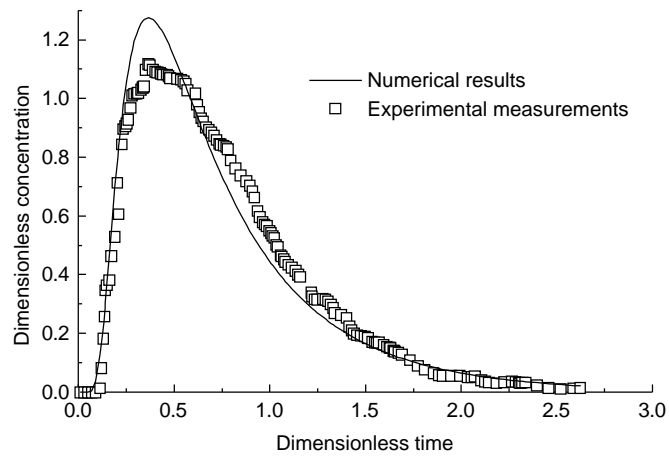


Fig. 9: Comparison of experimental results [9] and the simple vessel model using Eq. (10) and Eq. (9) (procedure 2).

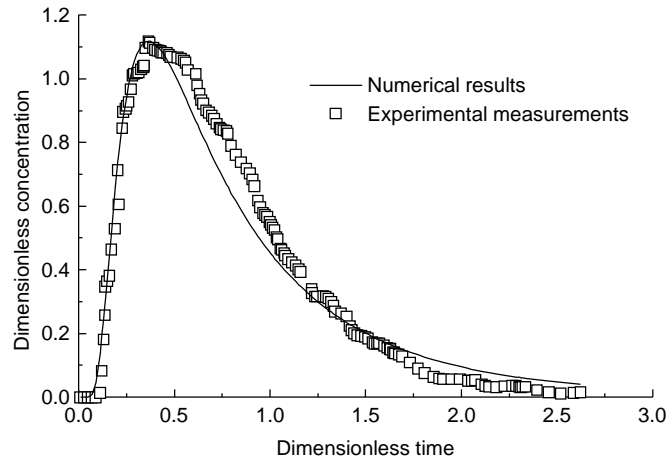


Fig. 10: Comparison of experimental results [9] and the simple vessel model using Eq. (11) and Eq. (8) (procedure 3).

#### IV A multivolume vessel model

The model described above succeeded in representing a variety of experimental RTD curves. However it fails to describe correctly RTD curves with two peaks. These curves arise when short circuits are present in the system [10]. Consequently a model consisting of two convection-diffusion volumes connected in parallel and a dead volume is proposed (Figure 11).

For a steady state problem where both the flow rate at the entrance of the vessel  $Q_{in}$ , and the flow rate at the exit of the vessel,  $Q_{out}$ , are constant in time, the following relations hold

$$Q_{in} = Q_{out} = Q^1 + Q^2 = Q \quad ; \quad Q_d = 0$$

The entrance tracer pulse is modeled by a Dirac's delta function

$$C_{in}(\mu) = C_{in}^1(\mu) = C_{in}^2(\mu) = \delta(\mu) \quad (13)$$

To calculate the dimensionless concentration at the exit of each of the convection-diffusion volumes, Equation (3) must be applied, with Eq. (13) as boundary condition. For volume  $i$  ( $i = 1; 2$ ) the following

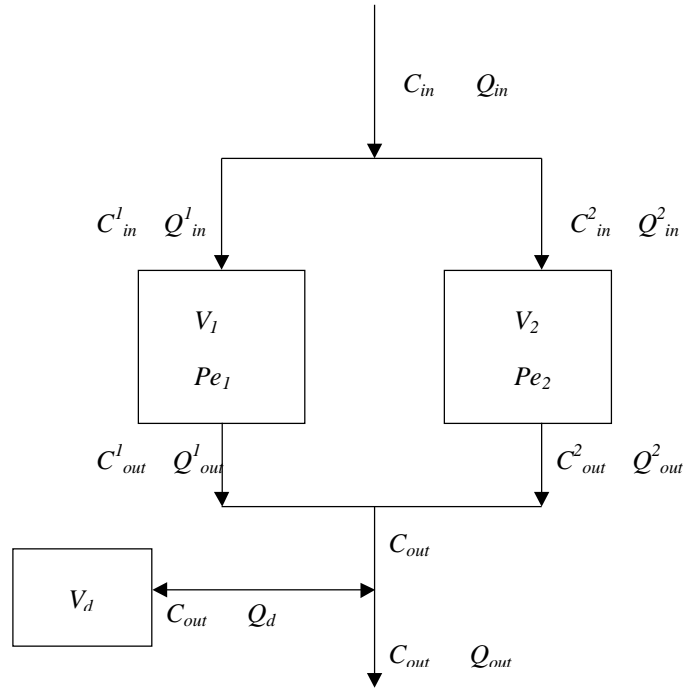


Fig. 11: Scheme of the multivolume tundish model.

expression is obtained

$$C_{out}^i(\mu) = \frac{q^i}{f_V^i} K_{Pe^i} \left[ 1 - \mu \frac{q^i}{f_V^i} \right]^{\mu}$$

where the relative flow rate  $q^i = Q^i/Q$  and the volume fraction  $f_V^i = V^i/V_T$  were introduced.

Finally the concentration exiting the system is obtained by tracer conservation which leads to the following expression

$$C_{out}(\mu) = \frac{q_1^{c_2}}{f_V^1} K_{Pe^1} \left[ 1 - \mu \frac{q_1}{f_V^1} \right]^{\mu} + \frac{q_2^{c_2}}{f_V^2} K_{Pe^2} \left[ 1 - \mu \frac{q_2}{f_V^2} \right]^{\mu} \quad (14)$$

This expression contains three dimensionless parameters,  $f_V^1$ ;  $f_V^2$ ;  $q^1$ ;  $Pe^1$  and  $Pe^2$  (the parameter  $q^2$  is given by  $q^2 = 1 - q^1$ ). All the parameters must be positive and the volume fractions must satisfy the inequality  $f_V^1 + f_V^2 \leq 1$ : Note that the dead volume influences the result indirectly by reducing the convection-diffusion region (otherwise  $f_V^1 + f_V^2 = 1$ ).

Any experimental RTD curve is expected to be well represented by Equation (14) if suitable values for the parameters are chosen. A numerical code (RESIDENCE [11]) was developed to find the set of parameters which minimizes (in a  $L^2$  sense) the distance between a given experimental curve and  $C_{out}(\mu)$ : This program

Case	Authors	V [l]	Q [l=s]	Vessel type	Figure
1	Barrón Meza et.al [8]	13:7	0:2066	one strand tundish	12
2	Zong et al [9]	30:0	0:0666	continuous re...ning vessel	13
3	Chakraborty et al[13]	186:3	0:5046	one strand tundish	14
4	Singh et al[10]	86:2	0:155	one strand tundish	15
5	Zong et al [9]	30:0	0:0666	continuous re...ning vessel	16

Table III: Different RTD curves considered for the validation of the model

Cases	$f_V^1$	$f_V^2$	$q^1$	$Pe_1$	$Pe_2$
1	0:00	1:00	0:00	1:00	5:26
2	0:23	0:54	0:23	12:12	4:00
3	0:29	0:71	0:42	3:03	5:63
4	0:87	0:025	0:87	3:59	6:64
5	0:0083	0:76	0:045	223:7	4:34

Table IV: Optimal values of the parameters.

was coded in Fortran and makes use of the IMSL subroutine DBCLSF, which solves nonlinear least squares problems using a modified Levenberg-Marquardt algorithm [12].

## A Validation of a multivolume vessel model

In order to validate the multivolume model, several experimental measurements found in literature are going to be considered. In Table III we present the different cases to be analyzed.

In Table IV we show the optimal values obtained by our program RESIDENCE [11] and in the Figures 12 to 16 we compare numerical results and experimental measurements.

Case 1 (Figure 12) has already been considered in the previous section and was matched with the simple model. From Table IV we see that the addition of a convection diffusion volume does not affect the results.

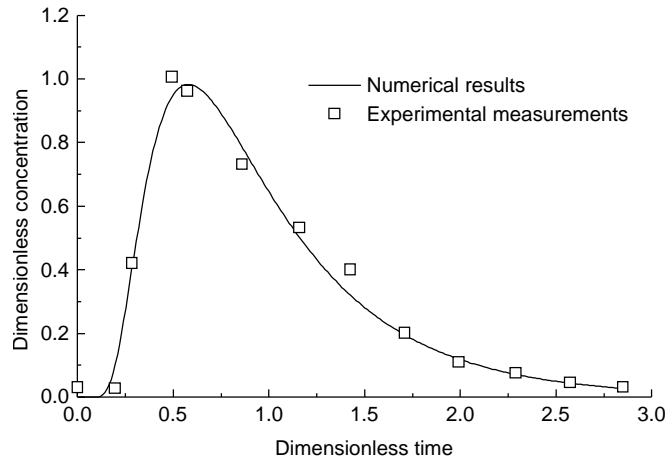


Fig. 12: Comparison of experimental results [8] and the multivolume vessel model.

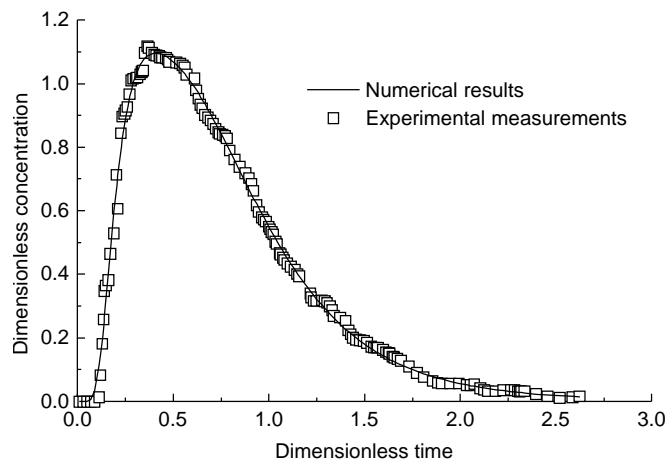


Fig. 13: Comparison of experimental results [9] and the multivolume vessel model.

Only one convection-diffusion volume was really needed, since both  $f_V^1$  and  $q^1$  vanish.

Case 2 (Figure 13) has also been addressed in the previous section. However in this case an improvement in the accuracy of the approximation was achieved by the multivolume model.

The third example, taken from Chakraborty and Sahai [13], is plotted in Figure 14. For this RTD curve, a traditional analysis becomes troublesome since numerical integration of the experimental data renders  $\mu_{av} > 1$ : However, the numerical results given by the multivolume vessel model show a reasonable agreement with the experimental points.

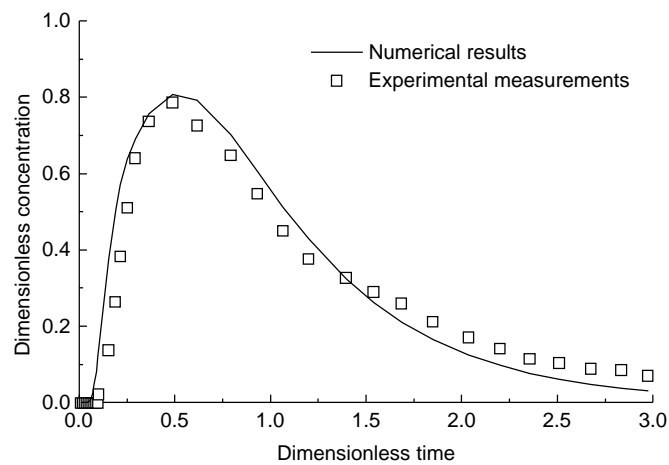


Fig. 14: Comparison of experimental results [13] and the multivolume vessel model.

Up to now we have presented examples of RTD curves with a single peak. In case 4 (Figure 15) we consider a two peaked RTD curve measured by Singh and Korla [10]. In this case each peak could be associated to a volume, the sharpest peak corresponding to the smallest volume: Obviously, this kind of curve could not be reasonably approximated by a single convection-diffusion volume.

Another example of two peaked RTD curve is shown in Figure 16. Experimental points were also taken from the work by Zong et al. [9] (with the water model described in the second example). Like the previous example, the extremely sharp peak due to a short-circuit is modeled by a very small convection diffusion volume,  $V_1$ ; with a high Péclet number.

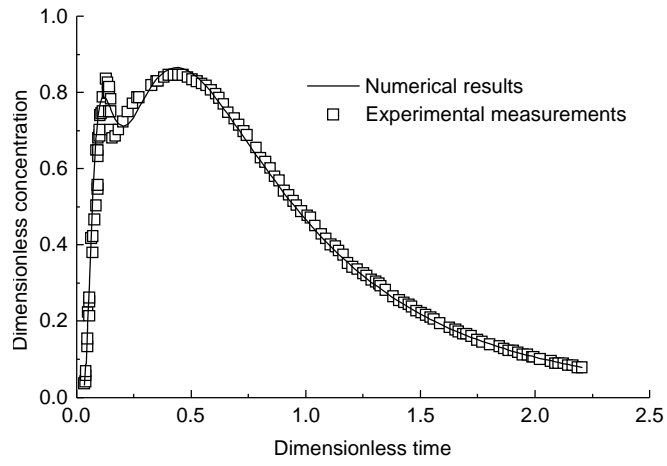


Fig. 15: Comparison of experimental results [10] and the multivolume vessel model.

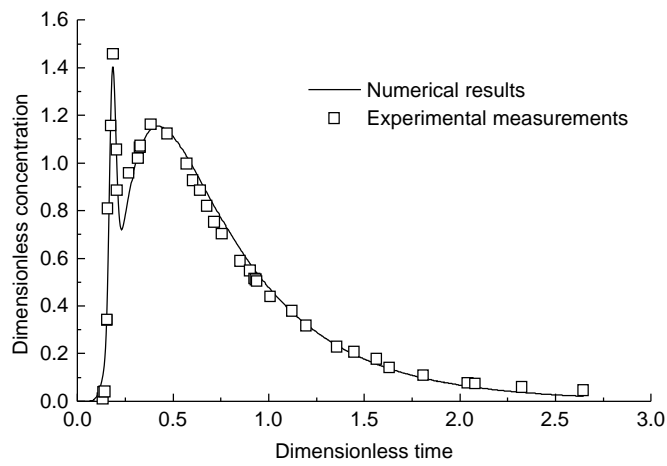


Fig. 16: Comparison of experimental results [9] and the multivolume vessel model.

## V Analysis of a multiple line tundish

We present an example corresponding to a four line tundish with the volume of 3.44 m<sup>3</sup> and a flow rate of 49:94 l/min in each line. In a multiple line tundish, it is of interest to model the RTD curve resulting from the addition of the RTD curves of each line [1].

In this example the RTD curves were obtained by the following procedure:

- 2 The liquid steel flow inside the tundish was calculated with a 3D numerical model using (k-L)-predictor / (")-corrector turbulent model (where k is the turbulent kinetic energy, " is the dissipation rate of k, and L is the mixing length). This numerical model was developed and tested in our previous publication [14]-[19]
- 2 Once the velocity field and turbulence variables were obtained, the tracer transport equation in a turbulent stream was calculated by solving a transient 3D turbulent convection-diffusion equation [20].

In the Figure 17 the internal and external lines of a symmetric four line tundish are shown, together with the global RTD curve. The approximation of the global RTD curve, also shown in Figure 17, is obtained using the multiple volume model described in section IV.

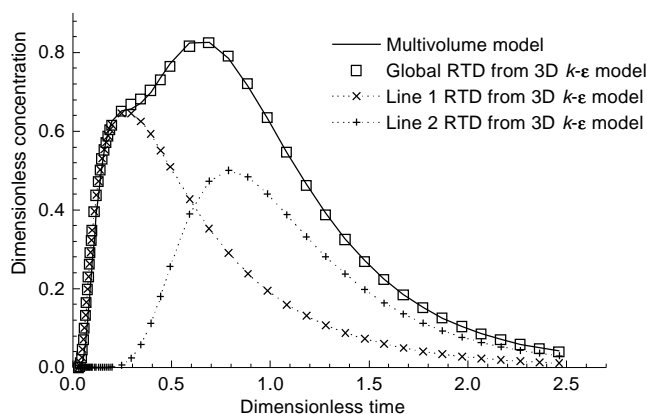


Fig. 17: Numerical results from a three dimensional model of a four line tundish compared to results from the present model

The values of the parameter obtained for this case are:  $f_V^1 = 0.56$  ;  $f_V^2 = 0.36$  ;  $q^1 = 0.54$ ;  $Pe_1 = 9.01$ ;  
 $Pe_2 = 1.96$

## VI Conclusions

Two numerical models for the simulation of RTD curves in different vessels are presented. The comparison of measured RTD curves with numerical results from the proposed models shows that these models can successfully represent the general behavior of the fluid inside a variety of systems. The RTD curves used for validation of the model include experimental data found in literature and numerical data obtained from a full three dimensional computation of the turbulent flow in a tundish.

The first of the models proved to be efficient to describe most of the one peaked RTD curves, in spite of its simplicity. The second one, slightly more complex, represented successfully all the different RTD curves under consideration, including those with two peaks.

The key feature of these models is the use of a new type of volume -the convection-diffusion volume- introduced in this work. The characteristics of this volume were deduced from the convection-diffusion one dimensional equation with a pulse boundary condition in the origin. For this reason, the use of convection-diffusion volume is not restricted to systems that exhibit small degree of mixing. This allows the representation of the different vessels with very simple models.

In order to find the parameters of the model for a given experimental RTD curve, a numerical algorithm was developed. We also found some simple mathematical relations that allow the estimation of the parameters of the model from the characteristic parameters of the RTD curve.

## List of Symbols

$a(\text{Pe})$	Area subtended by the origin and the peak of the curve in a RTD plot.[dimensionless]
$C$	Dimensionless concentration
$C_0$	Dimensionless concentration at the vessel entrance.
$C_p$	Dimensionless concentration of the peak of the RTD curve
$D$	Mean turbulent diffusivity [ $\text{mm}^2 = \text{sec}$ ]
$f_V^i$	Volume fraction [dimensionless]
$K_{\text{Pe}}$	Kernel associated to the convection-diffusion volume [dimensionless]
$\mathcal{K}_{\text{Pe}}$	Kernel developed by Levenspiel and Smith [6] [dimensionless]
$L$	Length of the 1D domain [mm]
$\text{Pe}$	Péclet number [dimensionless]
$q^i$	Relative flow rate [dimensionless].
$Q$	Flow rate in the vessel [ $\text{mm}^3 = \text{sec}$ ]
$v$	Mean velocity inside the 1D domain [mm/sec]
$v_a$	Active volume fraction [dimensionless].
$v_d$	Dead volume fraction [dimensionless].
$V$	Volume of the vessel [ $\text{mm}^3$ ]
$x$	Dimensionless coordinate along the flow direction.
$\mu$	Dimensionless time
$\mu_p$	Dimensionless time for the peak of the RTD curve
$\mu_{\text{av}}$	Average residence time [dimensionless].
$\zeta$	Theoretical residence time [sec]

## Acknowledgements

The authors would like to thank Dr. E. Dvorkin for his continuous support in numerical methods and Dr. Javier Etcheverry for his comments on some mathematical aspects of the paper.

This research was supported by SIDERCA (Campana, Argentina), SIDOR (Puerto Ordaz, Venezuela) and DALMINE (Bérgamo, Italy).

## References

- [1] D. Mazumdar and R. I. L. Guthrie, *ISIJ Int.*, 1999, vol 39, pp 524-547.
- [2] B.E. Launder and D. B. Spalding: *Comp. Meth. in Appl. Mech. And Engrg.*, 1974, vol. 3, pp. 269-289.
- [3] J. Szekely and N. J. Themelis: *Rate Phenomena in process metallurgy*, John Wiley & Sons Inc., New York, 1971, pp 515-555.
- [4] A.D. Martin, *Chem. Eng. Sci.*, 2000, Vol. 6, pp 5907-5917
- [5] Y. Sahai and R. Ahuja, *Ironmaking Steelmaking*, 1986, vol 13, pp 241-252.
- [6] O. Levenspiel and W. K. Smith, *Chem. Eng. Sci.*, 1957, vol. 6, pp 227-233.
- [7] O. Levenspiel: *Chemical Reaction Engineering*, John Wiley & Sons Inc., New York, 1972, pp 277-347.
- [8] M. A. Barrón-Meza, J. de J. Barreto-Sandoval and R.D. Morales, *Metalurgical and Material Transactions B*, 2000, vol 31B, pp 63-74.
- [9] J. Zong, K. Yi and J Yoon, *ISIJ Int*, 1999, vol. 39, pp 139-148.
- [10] S. Singh and S. Korla, *Steel Research*, 1995, Vol. 66, pp. 294-
- [11] *RESIDENCE user manual*, Center for industrial research, 2001.
- [12] IMSL (1994), *IMSL MATH/LIBRARY User's Manual*, Version 3.0, Visual Numerics, Inc., Houston, Texas.
- [13] S. Chakraborty and Y. Sahai, *Metalurgical Transactions B*, 1991, Vol. 22B, pp 429-437
- [14] M. B. Goldschmit and M. A. Cavaliere, *Appl. Mech. Rev.*, ASME, vol 48, n°11, part 2, 1995, pp S211-S215
- [15] M. B. Goldschmit and M. A. Cavaliere, *Engineering Computations*, 1997, vol 14, N° 4, pp 441-455.
- [16] M. B. Goldschmit, R. J. Príncipe y M. Koslowski, 3rd. *European Conference on Continuous Casting*, Madrid, Octubre 1998.

- [17] M. B. Goldschmit, 80th Steelmaking Conference, Chicago, EEUU, 1997.
- [18] M. B. Goldschmit, R. J. Principe and M. Koslowski, *Int. J. Numer. Meth. in Eng.*, 1999, vol. 46, 1505-1519.
- [19] M. Maldovan, J. Príncipe, G. Sánchez, A. Pignotti, and M. Goldschmit: ECCOMAS 2000, Barcelona
- [20] M. B. Goldschmit, S. P. Ferro, G. F. Walter, V. G. Aranda and J. A. Tena Morelos, *Metallurgical and Material Transactions B*, 2001, 32B, 537-546.